Keck Adaptive Optics Note 314

Measured field curvature at the Tip-tilt Sensor Stage focal plane

Antonin H. Bouchez, David Le Mignant

v3: May 05, 2005

1. Introduction

In order to maintain correct focus on the science camera during LGSAO observations, the tip-tilt sensor stage (TSS) must translate the low-bandwidth wavefront sensor (LBWFS) along a curved focal surface. The focal plane curvature predicted by a Zemax model of the telescope and AO bench has previously been presented in KAON 309[1]. This document describes measurements of the field curvature using both starlight and the fiber source, performed in January through May 2005.

Measurements on the sky record the effects of the field curvature of both the telescope and AO bench, while measurements on the fiber are sensitive only to the AO bench optics, plus possible misalignments of the fiber positioning stage (SFP). While the earliest sky and fiber measurements agreed to better than 25% (version 1 and 2 of this document), this is not the case with the most recent (28 April) sky measurements. They appear consistent with the TSS focal surface being described by the sum of the expected concave curvature[1] and a strong slope along the x-axis, most likely caused by misalignment of the TSS stage.

2. Field curvature measured on a star cluster

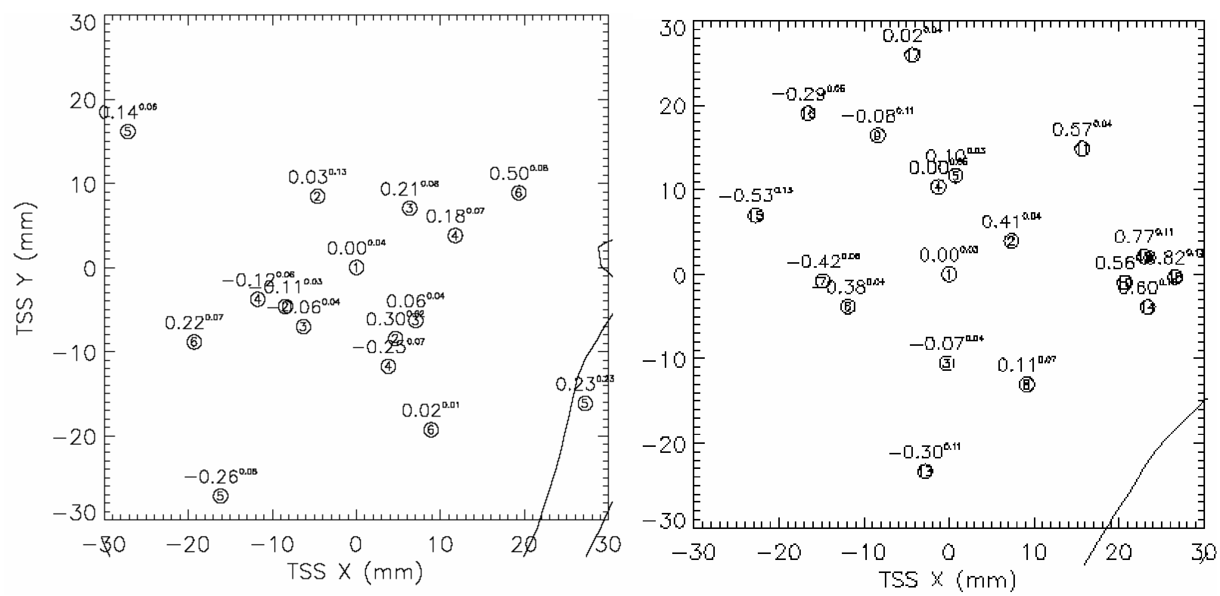

Figure 1: Focus in millimeters measured by the LBWFS on stars in the Orion Trapezium (*left*) and M11 (*right*). The star ID and focal plane position are indicated by the circled numbers. The focus is indicated above, with the 1-σ uncertainty in small font. Axes are labeled in device coordinates, relative to the optical axis. The 10 and 20% vignetting contours are also shown.

We observed the 6 brightest stars of the Orion Nebula Trapezium in dual NGS-STRAP mode for one hour on February 25, 2005. θ^1C Ori (V=5.14) was kept on the telescope optical axis, while the TSS x and y axes were driven to allow other

1 Wizinowich, P.W., KAON 309, January 2005.

bright stars to be viewed by STRAP and the LBWFS. The TSS z axis was kept fixed at the nominal optical axis focus position. For each star, the tip-tilt loop was closed on STRAP, the high-order loop closed on the fast wavefront sensor (WFS), and 3 images taken with the LBWFS. This experiment was repeated with the rotator in three positions (PA = 0, 90, 180), allowing the LBWFS to measure the apparent focus and high-order aberrations at 16 locations across the TSS focal plane. The measured focus values versus TSS x and y position are shown in Figure 1. A positive value of LBWFS focus implies that the focus is *behind* the camera field stop.

The same experimental procedure was repeated on 23 bright stars in the M11 open cluster on 28 April, 2005. Due to the large number of stars available in this cluster, only one position angle was observed. LBWFS focus measurements were far more consistent in this second experiment, probably due to a more stable atmosphere (seeing ~0.5" at K) and the lack of a varying nebular background. M11 proved to be an ideal target for this experiment. The test procedure and list of stars used in this experiment are given in Appendix A.

3. Field curvature measured on the AO fiber

Similar experiments using the fiber source were performed on 12 January 2005 and 25 April 2005. In these experiments, the fiber was translated by the SFP across the focal plane in a 25x25 or 20x20 grid centered on the optical axis, while the SFP z axis was kept at the nominal optical axis focus position. The TSS was moved in x and y by the equivalent amount, to allow the LBWFS to image the fiber at each position. The TSS z axis was kept at the nominal optical axis focus position. The measured LBWFS focus as a function of TSS x and y position is shown in Fig. 2. Grid points for which the vignetting was greater than 10% have been excluded from the plot and the subsequent analysis. The reduced vigneting of the TSS stage in April, subsequent to work on the AO bench by P. Wizinowich and R. Sumner, is apparent.

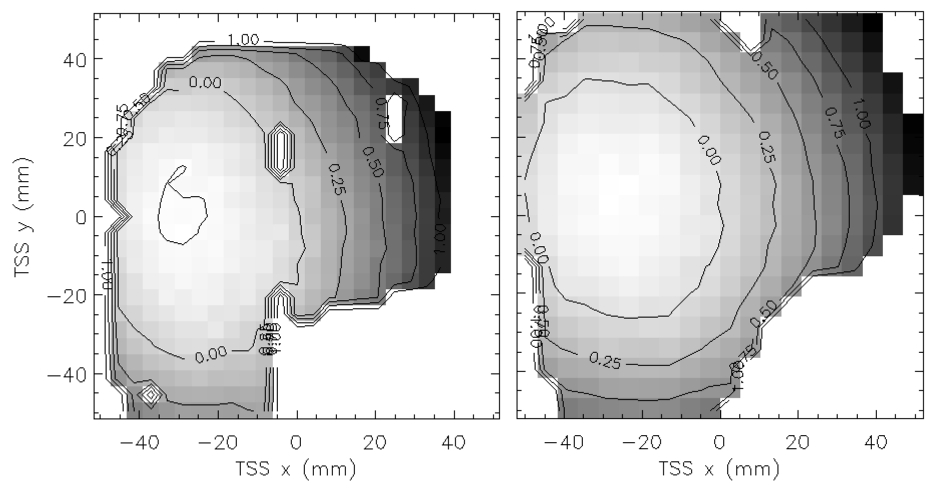

Figure 2: Focus in millimeters measured with the LBWFS on the AO fiber. Axes are labeled in device coordinates, relative to the optical axis. *Left:* 12 January 2005. *Right:* 25 April 2005.

4. Field curvature model in device coordinates

Earlier versions of this document present polynomial fits to the January fiber and February sky data. These earlier experiments are ignored in the analysis which follows, since the more recent experiments sampled a larger region of the focal plane and, in the case of the April stellar observations, are more sensitive. A polynomial surface of the form $z = \Sigma\, k_{ij}\, x^i\, y^j$ was fit to the April fiber and sky data using a weighted least-squares approach. The best-fit coefficients for first and second-order fits are listed in Table 1.

i	j	k_{ij} sky (1st order)	k_{ij} sky (2nd order)	k_{ij} fiber (1st order)	k_{ij} fiber (2nd order)

1	0	0.0300861	**0.0299479**	0.0122802	0.00171922
0	1	0.00656687	**0.00819109**	0.000183775	-0.0143817
1	1	0	**1.61598E-05**	0	2.43337E-05
2	0	0	**-4.97629E-05**	0	2.50176E-04
0	2	0	**-1.67673E-04**	0	2.87090E-04

Table 1: Coefficients of the best 1st and 2nd-order polynomial fit to the sky and fiber data.

Figure 3 compares the field curvature models fit to the sky and AO fiber, and that predicted by the optical model. All three models are quite different. The fiber data shows a convex curvature (with respect to the incoming light) which is not present in the sky data or the optical model, while the sky data shows a strong positive slope along the TSSx axis. The sky data are nearly consistent with a planar fit (see Figure 4). However, the slight concave curvature of the second-order fit to the focal surface suggests that the best model may be the field curvature predicted by the optical model, plus a slope due to misalignment of the TSS stage.

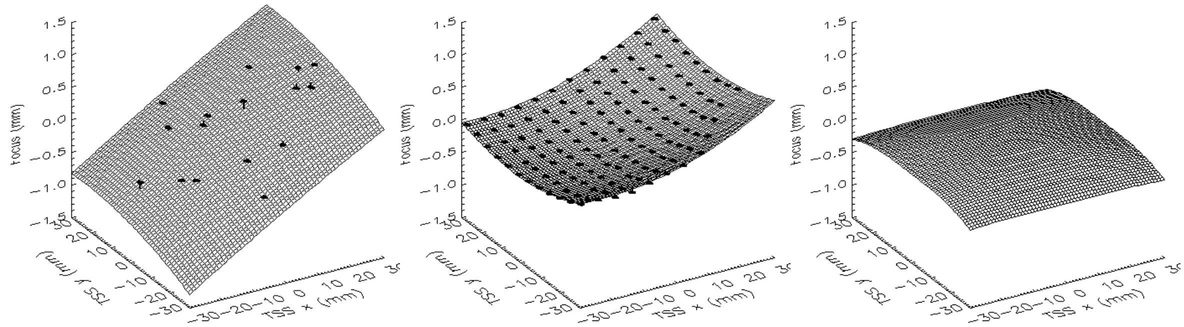

Figure 3: *left:* Second-order model fit to the April sky data. Measurements are shown as points, connected to the surface by vectors. *center:* Second-order model fit to the April fiber data. *right:* Field curvature expected from the optical design[1]. All are displayed on the same scale, with light traveling in the +z direction.

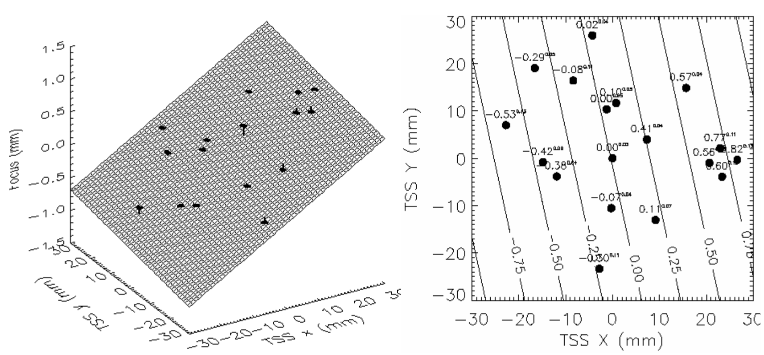

Figure 4: First-order model fit to the April sky data. Focus values are in millimeters.

5. Conclusions

The April 28, 2005 observations of M11 lead us to draw a significantly different conclusion from the first two versions of this report. These more recent on-sky data are of sufficient quality to demonstrate that measurements of the off-axis focus using the AO fiber do not record the true focus position. Instead, the on-sky data suggest that the focal surface seen by the STRAP and LBWFS is dominated by a slope in the +TSSx direction, probably due to misalignment of the TSS stage. We recommend that until the stage is realigned, the 2nd order polynomial model described by the bold font coefficients in Table 1 be implemented to drive the sensors along this sloped and slightly concave surface.

Appendix A: Starlist and software

The starlist and test procedure used for the 28 April, 2005 experiment are listed below. The test uses the IDL program TSSFOCUSTEST on k2aoserver to move between stars and gather all the necessary data.

Procedure: /home/k2ao/RUNS/050428/tss_foc_test_050428.doc

Starlist: /kroot/starlists/nirc2eng/ngs050428_m11.lst

```
m11_2142        18 51  7.964 -06 16 43.41 2000.0 vmag=8.50 sep=0.1
m11_899         18 51  8.331 -06 16 53.52 2000.0 vmag=11.74 sep=11.5
m11_948         18 51  6.992 -06 16 43.03 2000.0 vmag=13.37 sep=14.4
m11_2150        18 51  8.922 -06 16 41.66 2000.0 vmag=12.63 sep=14.5
m11_879         18 51  9.044 -06 16 44.43 2000.0 vmag=12.26 sep=16.2
m11_926         18 51  7.611 -06 16 27.01 2000.0 vmag=11.37 sep=17.2
m11_915         18 51  7.889 -06 16 22.95 2000.0 vmag=13.50 sep=20.5
m11_960         18 51  6.759 -06 16 56.04 2000.0 vmag=13.19 sep=21.9
m11_854         18 51  9.484 -06 16 31.83 2000.0 vmag=11.19 sep=25.5
m11_916         18 51  7.877 -06 17 11.88 2000.0 vmag=11.62 sep=28.5
m11_867         18 51  9.341 -06 17  4.99 2000.0 vmag=12.55 sep=29.8
m11_905         18 51  8.163 -06 17 15.06 2000.0 vmag=13.71 sep=31.8
m11_997         18 51  5.805 -06 16 39.56 2000.0 vmag=11.84 sep=32.4
m11_927         18 51  7.606 -06 17 15.62 2000.0 vmag=13.20 sep=32.6
m11_890         18 51  8.609 -06 16 12.05 2000.0 vmag=13.24 sep=32.8
m11_847         18 51  9.725 -06 16 20.52 2000.0 vmag=13.74 sep=34.9
m11_818         18 51 10.365 -06 16 37.44 2000.0 vmag=13.75 sep=36.4
m11_2141        18 51  7.936 -06 17 20.08 2000.0 vmag=11.57 sep=36.7
m11_1004        18 51  5.587 -06 16 59.19 2000.0 vmag=11.83 sep=38.7
m11_838         18 51  9.950 -06 17 11.14 2000.0 vmag=13.60 sep=40.6
m11_1030        18 51  5.012 -06 16 41.41 2000.0 vmag=12.52 sep=44.0
m11_791         18 51 10.878 -06 16 29.21 2000.0 vmag=12.94 sep=45.8
m11_942         18 51  7.101 -06 17 28.22 2000.0 vmag=11.28 sep=46.6
m11_988         18 51  5.984 -06 16  7.26 2000.0 vmag=12.95 sep=46.6
m11_1001        18 51  5.776 -06 17 17.19 2000.0 vmag=12.66 sep=46.9
m11_1031        18 51  4.951 -06 17  2.63 2000.0 vmag=13.54 sep=48.8
m11_1021        18 51  5.136 -06 16 18.06 2000.0 vmag=12.66 sep=49.1
```